# Communications to the Editor

## Test of the Foundations of Classical Rubber Elasticity

**Ralf Everaers* and Kurt Kremer**

*Theorie II, Institut für Festkörperforschung, Forschungszentrum Jülich, Postfach 1913, D-52425 Jülich, Germany*

*Received February 8, 1995*
*Revised Manuscript Received June 13, 1995*

**Introduction.** The classical theories of rubber elasticity[1−9] provide a simple and at least qualitatively successful explanation of the entropic elasticity of these materials. Their fundamental assumption is that **(I)** the elastic response of the network is composed of contributions of the individual network strands, which may be treated as independent entropic springs. For moderate extensions these springs can be regarded as harmonic due to the Gaussian distribution of the end-to-end vector $\vec{R}$ of flexible polymers in a melt:

$$p(x,y,z) = p(x)\,p(y)\,p(z) \tag{1}$$

$$p(x) = \left(\frac{3}{2\pi\langle R^2\rangle}\right)^{1/2} \exp\left(-\frac{3x^2}{2\langle R^2\rangle}\right) \tag{2}$$

In principle, assumption I holds only for a network of phantom chains which may pass freely through their neighbors and themselves. In real networks the strands are impenetrable and highly entangled. The classical theories disregard the topological constraints[10,11] on the strand conformations beyond the position fluctuations of the cross-links. The purpose of the present paper is to—to our knowledge for the first time—*quantify* the error introduced into the calculation of the elastic properties by this widely used assumption.[1−9,12,13]

Our conclusions are based on microscopic information available *only* in a computer simulation.[14,15] We use molecular dynamics (MD) simulations to investigate model polymer networks under elongational strain. This allows us to *simultaneously* determine the true shear moduli from the restoring forces *and* the classical prediction for these moduli from the change in the network strand elongations. Our analysis does not involve any adjustable parameters and directly tests assumption I.

The experimental evidence for the validity of the classical approach is controversial and largely indirect. Classical predictions for experimental systems contain parameters related to the lack of microscopic information on **(II)** the connectivity of the network (i.e., the densities of *elastically active* strands $\varrho_{\text{strand}}$ and cross-links $\varrho_{\text{cross}}$ or of the cycle rank $\xi$),[16] **(III)** the end-to-end distance distribution $p_{\text{strand}}(\vec{r})$ of the network strands in the unstrained state, and **(IV)** the change of this distribution upon deformation of the sample. Attempts to *independently* determine the model parameters indicated from early on that the classical theories underestimate the modulus.[17] Computer simulations[14] and experiments[18] on end-linked model networks find that the shear modulus extrapolates to a *finite* value in the limit of infinite strand length, a result which is irreconcilable with any classical theory. Finally, SANS data for deuterated paths through a strained, cross-linked melt do not support the classical picture of independently relaxing network strands[19] but rather the tube model.[20] In contrast to all these findings, there is a wealth of seemingly positive evidence from fitting experimental stress−strain curves. The constrained junction models,[5−9] in particular, have been shown to provide an excellent parametrization of experimental data.[21,22] Note, however, that a formally identical expression can be derived from the slip-link model[23] and that the data can often be described as well by expressions derived from tube models.[24] The capability of the constrained junction models to reproduce the *shape* of stress−strain curves seems therefore insufficient to justify assumption I.

**Randomly Interpenetrating Polymer Networks with Diamond Lattice Connectivity.** A randomly cross-linked melt of linear polymers has a highly irregular connectivity. Typical defects are polydispersity, dangling ends and clusters, and self-loops. While these imperfections can be analyzed in the framework of the phantom model,[12,16] they are a serious complication in a study of the consequences of topology conservation. "Chemically" defect-*free* polymer networks with the connectivity of a crystal lattice[3] can only be generated in a computer simulation. We quench the topology from a state where $n$ diamond networks with typical phantom network conformations interpenetrate each other randomly. The conformational statistics of the unstrained state are not affected by the topology quench and can be derived from the phantom model.

Phantom networks collapse unless this is prevented by fixing the positions of cross-links on the surface[2] or, as in this work, by introducing periodic boundary conditions.[25] In our study each of the $n$ networks is composed of 128 strands and corresponds to $2 \times 2 \times 2$ unit cells of a diamond lattice. Comparisons to systems corresponding to $3 \times 3 \times 3$ unit cells did not reveal significant finite size effects.[26] In the spirit of the Flory−Rehner model[27] we chose the magnitude of the bond vector $\vec{r}_1$ (the subscript denotes the sample elongation $\lambda = 1$) equal to the root-mean-square (rms) end-to-end distance $\langle R^2\rangle^{1/2}$ of un-cross-linked strands in a melt. For Gaussian chains eq 1 holds for $p_{\text{strand}}(\vec{r})$ due to the symmetry of the diamond lattice. It is convenient to consider $p_{\text{strand}}(x)$, etc., for each Cartesian component separately.

For a regular phantom network the mean positions of the cross-links are identical to the lattice sites.[3] Each strand has the same, nonzero mean extension equal to the bond length of the lattice; i.e., the distribution of the *mean* strand end-to-end distances is given by $p^{\text{mean}}_{\text{strand}}(x) = {}^1/_2(\delta(x - x_1) + \delta(x + x_1))$ with $x_1 = (1/\sqrt{3})|\vec{r}_1|$. Note that in order to determine this distribution for a randomly cross-linked melt it is necessary to know $\varrho_{\text{strand}}$ and $\varrho_{\text{cross}}$ or equivalently the cycle rank $\xi$.[4,28] In a phantom network with four-functional cross-links the strand extensions fluctuate around their mean

0024-9297/95/2228-7291$09.00/0 

values by an amount of $\Delta^2 = {}^1/_2\langle R^2\rangle^{1/2}$.[4,28] For our particular choice of the lattice constant we expect for the vector $\vec{\Delta}_1$ of fluctuation widths in the three spatial dimensions $|\vec{\Delta}_1|^2 = {}^1/_2|\vec{r}_1|^2$. The strand end-to-end distance distribution at any particular instant in time is given by the convolution of $p_{\text{strand}}^{\text{mean}}(x)$ with the normally distributed fluctuations,[4] yielding a superposition of two symmetric Gaussian peaks of width $\Delta_{1x} = (1/\sqrt{3})|\vec{\Delta}_1|$ around $x_1$:

$$p_{\text{strand}}(x) = \frac{1}{2}\frac{1}{\sqrt{2\pi}\Delta_{1x}}\left(\exp\left(-\frac{(x-x_1)^2}{2\Delta_{1x}{}^2}\right) + \exp\left(-\frac{(x+x_1)^2}{2\Delta_{1x}{}^2}\right)\right) \quad (3)$$

For future reference we note that the entropy density of an ensemble of strands with a distribution (3) is given by

$$S(\vec{r},\vec{\sigma}) = S_0 - \varrho_{\text{strand}}\frac{3k_B}{2\langle R^2\rangle}(\vec{r}^2 + \vec{\Delta}^2) \quad (4)$$

**Classical Predictions for the Shear Modulus.** In the following we will discuss the predictions of the phantom and the affine model for the elastic response of diamond networks to a simple, volume-conserving elongation.[29] The more sophisticated constrained junction models[5-9] interpolate between these two limits.

In the phantom model[2-4] the fluctuations are strain independent and only the *mean* positions and distances of the cross-links change affinely with the outer dimension of the sample, i.e., $\vec{r}_\lambda = \hat{\lambda}\vec{r}_1$ and $\vec{\Delta}_\lambda = \vec{\Delta}_1$. The normal tension $\sigma$ in the sample introduced by the deformation is calculated from the change in the free energy density for the ensemble of network strands:

$$T\Delta S = \frac{1}{2}G(3 - \lambda^2 - 2\lambda^{-1}) \quad (5)$$

$$\sigma = G(\lambda^2 - \lambda^{-1}) \quad (6)$$

$$G_{\text{ph}} = \varrho_{\text{strand}}k_BT\frac{\vec{r}_1{}^2}{\langle R^2\rangle} = \varrho_{\text{strand}}k_BT \quad (7)$$

Equations 5 and 6 describing the mechanical behavior with a single parameter, the shear modulus $G$, hold generally for the small strain limit of all classical models and are well established by experiments.[1] The particular value for the phantom model prediction $G_{\text{ph}}$ of the shear modulus (eq 7) is characteristic for our diamond networks.

The classical view of entanglements[5-9] is to assume that their main effect is a partial suppression of the junction fluctuations compared to the phantom model. Ultimately, this ansatz leads to the affine model,[1] which therefore constitutes an *upper limit* for the modulus predicted from a classical theory. In this model junction positions (and hence their distances and $p_{\text{strand}}(\vec{r})$) change affinely with the outer dimension of the sample. For our particular systems this means $\vec{r}_\lambda = \hat{\lambda}\vec{r}_1$, $\vec{\Delta}_\lambda = \hat{\lambda}\vec{\Delta}_1$ and

$$G_{\text{aff}} = \varrho_{\text{strand}}k_BT\frac{\vec{r}_1{}^2 + \vec{\Delta}_1{}^2}{\langle R^2\rangle} = \frac{3}{2}\varrho_{\text{strand}}k_BT \quad (8)$$

**Table 1. Strand Length, Total Number of Particles, Energy per Particle in the Strained and Unstrained State, and the Measured, Classical, Phantom, and Affine Shear Moduli for the Systems under Investigation**

| $N$ | $N_{\text{mon}}$ | $U/N_{\text{mon}}$ [$k_BT$] | | $G$ [$\epsilon/\sigma^3$] | $G_{\text{class}}$ [$\epsilon/\sigma^3$] | $G_{\text{ph}}$ [$\epsilon/\sigma^3$] | $G_{\text{aff}}$ [$\epsilon/\sigma^3$] |
|---|---|---|---|---|---|---|---|
| 12 | 8000 | 2.4700 | 2.4704 | $0.100 \pm 0.003$ | 0.068 | 0.072 | 0.100 |
| 26 | 23744 | 2.4675 | 2.4672 | $0.060 \pm 0.003$ | 0.038 | 0.035 | 0.051 |
| 44 | 51264 | 2.4662 | 2.4660 | $0.041 \pm 0.002$ | 0.027 | 0.020 | 0.029 |

The ratio $G_{\text{aff}}/G_{\text{ph}} = {}^3/_2$ is an artefact of our choice of $\langle R^2\rangle^{1/2}$ for the bond length of the diamond lattice. In general, for an $f$-functional lattice one recovers the standard relation $G_{\text{aff}}/G_{\text{ph}} = f/(f-2)$ by setting $\vec{r}_1{}^2 = [(f-2)/f]\langle R^2\rangle$.

**The Simulation Model.** We use the same coarse-grained model as in earlier investigations of polymer melts and networks.[14,30] The polymers are modeled as freely jointed bead–spring chains of uniform length $N$. There are two types of interactions, an excluded-volume interaction, $U_{\text{LJ}}$, between all monomers and a bond potential, $U_{\text{FENE}}$, between chemical nearest neighbors. $U_{\text{LJ}}$ is a truncated Lennard-Jones potential. With $\epsilon$ and $\sigma$ as the LJ units of energy and length, we work at a temperature $k_BT = 1\epsilon$ and at a density $\varrho = 0.85\sigma^{-3}$ as in the other studies. The unit of time is $\tau = \sigma(m/\epsilon)^{1/2}$ with a monomer mass $m = 1$. The average bond length is $l = 0.97\sigma$ and $\langle R^2\rangle(N) \approx 1.7l^2N$. Topology is conserved, and the dynamics is dominated by the melt entanglement length, $N_e = 35$ monomers, and the Rouse time, $\tau_{\text{Rouse}} \approx 1.5N^2\tau$.[30] We carried out MD simulations where the system was weakly coupled to a heat bath and integrated in time steps of $0.01\tau$. The program was vectorized for the Cray YMP along the lines of the grid search algorithm.[31]

The $N$-monomer strands were cross-linked by four-functional monomers into networks with the connectivity of a diamond lattice and placed in a commensurable, cubic simulation box with periodic boundary conditions. The density of elastically active strands is given by $\varrho_{\text{strand}} = \varrho/(N + 1/2)$. The bond length of the diamond lattice was set to $\langle R^2(N+1)\rangle^{1/2}$ of the melt chains.[27] The diamond networks were prepared and relaxed as phantom networks with the correct melt persistence length.[14] To reach melt density, we superimpose $n \sim N^{1/2}$ diamond networks in the simulation volume. As in realistic systems there are on the order of $N^{1/2}$ cross-links in the volume of one chain. The excluded-volume interaction is switched on slowly to build up the monomer packing and eventually quench the topology. Note (a) that it is topology conservation and *not* the the screened excluded-volume interaction that causes the deviations from the classical behavior[26,32] and (b) that due to the regular network structure the longest relaxation times in the system are expected to be on the order of the Rouse times of the strands.

We have investigated systems with strand lengths $N = 12$, 26, and 44 (Table 1). The system sizes range from 8000 to 51 264 particles with $n = 5$, 7, and 9 subnets. The same samples were simulated first in the unstrained state and subsequently elongated[29] by typically 50%. Deformations were implemented as a short sequence of small step changes in the metrik $\hat{\lambda}^T\hat{\lambda}$ at the beginning of the runs. We measured the pressure tensor, $\hat{P}$, and watched the relaxation of the normal tension $\sigma = P_{xx} - {}^1/_2(P_{yy} + P_{zz})$ to a plateau value (inset in Figure 1). The stress relaxation was completed after a period of about $2\tau_{\text{Rouse}}$ compared to our overall simulation times on the order of $10\tau_{\text{Rouse}}$. For our largest

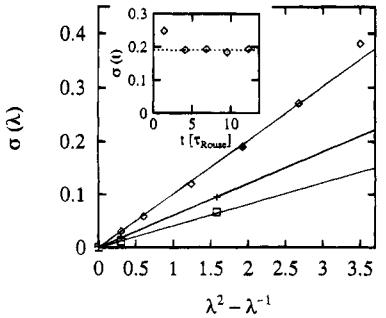


**Figure 1.** Stress–strain relations for stretched model networks: $N = 44$ (□), $N = 26$ (+), $N = 12$ (◇). The inset shows the stress relaxation after a step deformation. The corresponding data point in the full figure is marked by the dotted ◆.

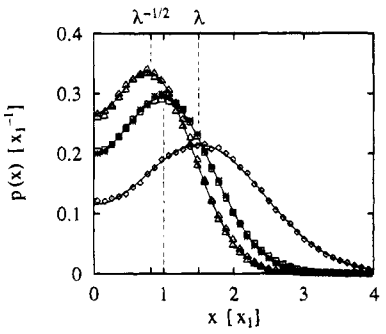


**Figure 2.** End-to-end distance distributions of network strands for $N = 44$ in the unstrained (□) and strained states (|| ◇ and ⊥ △). For comparison we have included data from the phantom runs before the introduction of the excluded-volume interaction (*). Distances are measured in units of the diamond lattice bond length. We have indicated the (affinely displaced) positions of the Gaussian peaks by horizontal lines. Note that the maxima of the curves have slightly different locations due to the superposition of peaks at $\pm x_1$.

systems this is equivalent to $8 \times 10^{10}$ particle updates. Data from the initial relaxation period were discarded for the analysis of conformational properties.

**Shear Moduli of Purely Entropic Origin.** Shear moduli were determined from the plateau values of the normal tension, which is equivalent to measuring restoring forces in stretching experiments. Figure 1 shows that our systems follow the typical stress–strain relation (6) for rubberlike materials. This allows us to determine the shear moduli $G$ listed in Table 1 with high accuracy from the slope of a straight line. Since the internal energies in the strained and in the unstrained state are identical (Table 1), our systems are *ideal model rubbers with purely entropic elasticity* and a valid test case for the foundations of rubber elasticity theory.

**Strand Elongations.** Figure 2 shows examples of the observed end-to-end distance distributions $p_{\text{strand}}(x)$, etc., for strained and unstrained samples. In all cases our data are well described by the superposition of two symmetric Gaussian peaks (eq 3). Fit parameters are listed in Table 2.

Note first that in the unstrained state the distributions are indeed identical for runs with and without excluded-volume interaction and topology conservation. The peak positions are identical to the chosen bond lengths of the diamond lattice. For longer chains we observe the expected values for the distribution width $\bar{\Delta}$, while the 10% discrepancy in the $N = 12$ case indicates deviations from the ideal Gaussian behavior.

For strained samples the strand elongations change as pictured by the constrained junction models. The peak positions transform affinely. The distribution widths $\bar{\Delta}_\lambda$ show a behavior intermediate between the phantom and the affine model limits, with a tendency toward the affine limit with increasing strand length $N$.

**Table 2. Fit Results for the Description of the End-to-End Distance Distribution by Equation 3**

| | | peak $\bar{r}$ | | width $\bar{\Delta}$ | |
|---|---|---|---|---|---|
| $N$ | $\lambda =$ | 1.0 | 1.5 | 1.0 | 1.5 |
| 12 | $x$ | 2.71 | 4.34* | 1.64 | 1.78* |
| | $y$ | 2.70 | 2.11* | 1.70 | 1.63* |
| | $z$ | 2.69 | 2.13* | 1.69 | 1.51* |
| 26 | $x$ | 3.87 | 5.84 | 2.62 | 3.27 |
| | $y$ | 3.83 | 3.10 | 2.55 | 2.28 |
| | $z$ | 3.81 | 3.11 | 2.72 | 2.37 |
| 44 | $x$ | 4.92 | 7.41 | 3.42 | 4.58 |
| | $y$ | 4.92 | 4.07 | 3.41 | 2.95 |
| | $z$ | 4.91 | 4.02 | 3.34 | 3.04 |

[a] The results for $N = 12$ marked by asterisks refer to runs with $\lambda = 1.6$.

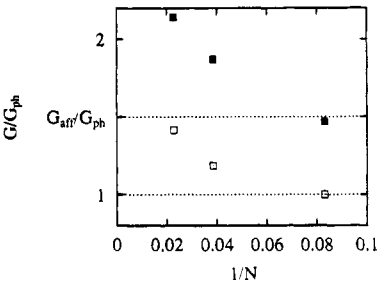


**Figure 3.** Strand-length dependence of the shear modulus normalized to the phantom model prediction $G_{\text{ph}}$ (eq 7). The filled symbols represent the measured values $G/G_{\text{ph}}$, and the open symbols indicate the classical prediction $G_{\text{class}}/G_{\text{ph}}$. $G_{\text{aff}}/G_{\text{ph}} = {}^3/_2$ (eqs 7 and 8) is the upper limit for any classical theory.

**Comparison of Measured and Predicted Moduli.** The parameter-*free* classical predictions $G_{\text{class}}$ for the shear moduli of our systems follow from differences in the strand elongations between the strained and unstrained state. In the framework of the classical theories these differences correspond to an entropy change that can be calculated from eq 4 using the parameters from Table 2. $G_{\text{class}}$ follows from eq 5. Our results for $G_{\text{class}}$, $G_{\text{ph}}$, $G_{\text{aff}}$, and the true modulus $G$ are listed in Table 1. A comparison shows that *the true change in entropy in a deformed network with conserved topology is significantly larger than that calculated from the strand elongations alone.* In Figure 3 we have plotted the ratios of $G/G_{\text{ph}}$ and $G_{\text{class}}/G_{\text{ph}}$ versus the inverse strand length $1/N$. The value $G_{\text{aff}}/G_{\text{ph}} = {}^3/_2$ (eqs 7 and 8) indicates the upper limit for a classical theory. The figure illustrates that the constrained junction models correctly anticipate the crossover of $G_{\text{class}}$ toward the affine limit for large strand lengths. However, they do not provide a reliable approximation for the true modulus $G$. For example, for $N = 44$, $G \gg G_{\text{aff}} > G_{\text{class}}$ and the observed increase of the modulus due to topology conservation from $G_{\text{ph}}$ is 3 times larger than expected from the classical ansatz.

**Moduli for Large Strand Lengths.** A rough estimate yields $G(N \to \infty) = 0.018 \pm 0.03\ \epsilon/\sigma^3$, compatible with recent simulation results for end-linked melts.[14] This suggests that the nonclassical effects (a) are of similar origin in both systems, (b) dominate for large $N$ with $\lim_{N\to\infty} G/G_{\text{class}} \to \infty$, and (c) cannot be explained by the recently developed constrained chain model[33]

which predicts a maximal shear modulus of $3G_{ph}$ for tetrafunctional networks.

**Summary and Conclusion.** The classical theories of rubber elasticity[1-9] are based on the assumption that the elastic response of the network is a single chain effect, due only to the elongation of the network strands. We have tested this assumption in molecular dynamics simulations of model polymer networks with conserved topology under elongational strain. We found (a) that macroscopically our systems behave as ideal model rubbers with a purely entropic elasticity and exhibit the classical stress–strain relation (6), (b) that microscopically the changes in the strand elongations upon deformation of the samples show the behavior anticipated by the constrained junction models, but (c) that *the true shear moduli G of the networks are significantly larger than the classical predictions $G_{class}$ calculated from the strand statistics alone. We conclude that, contrary to the Flory view, the contribution of topological constraints to the shear modulus of polymer networks cannot be estimated from the reduction of the junction fluctuations.* We believe that computer simulations will be crucial in the development of a more complete theory of rubber elasticity, be it based on topological invariants,[10,11,25,34,35] slip links,[35-37] or the tube model.[38-40] The interpretation of the topology contribution $G - G_{ph}$ to the modulus in terms of discrete loop entanglements[35] will be the subject of a forthcoming publication.

**Acknowledgment.** Discussions with G. S. Grest are gratefully acknowledged. This work was supported by a generous CPU time grant from the German Supercomputer Center HLRZ (Jülich) within the Disordered Polymer Project and by a NATO travel grant (No. 86680). R.E. acknowledges partial support from SFB262 of the Deutsche Forschungsgemeinschaft (DFG).

## References and Notes

(1) Treloar, L. R. G. *The Physics of Rubber Elasticity*; Oxford University Press: Oxford, U.K., 1975.
(2) James, H.; Guth, E. *J. Chem. Phys.* **1943**, *11*, 455.
(3) James, H. *J. Chem. Phys.* **1947**, *15*, 651.
(4) Flory, P. J. *Proc. R. Soc. London, Ser. A* **1976**, *351*, 351.
(5) Ronca, G.; Allegra, G. *J. Chem. Phys.* **1975**, *63*, 4990.
(6) Flory, P. J. *J. Chem. Phys.* **1977**, *66*, 5720.
(7) Erman, B.; Flory, P. J. *J. Chem. Phys.* **1978**, *68*, 5363.
(8) Flory, P. J.; Erman, B. *Macromolecules* **1982**, *15*, 800.
(9) Kästner, S. *Colloid Polym. Sci.* **1981**, *259*, 499, 508.
(10) Edwards, S. F. *Proc. Phys. Soc.* **1967**, *91*, 513.
(11) Edwards, S. F. *J. Phys. A* **1968**, *1*, 15.
(12) Higgs, P. G.; Ball, R. C. *J. Phys. Fr.* **1988**, *49*, 1785.
(13) Goldbart, P. M.; Zippelius, A. *Phys. Rev. Lett.* **1993**, *71*, 2256.
(14) Duering, E. R.; Kremer, K.; Grest, G. S. *Macromolecules* **1993**, *26*, 3241; *J. Chem. Phys.* **1994**, *101*, 8169.
(15) Everaers, R.; Kremer, K.; Grest, G. S. *Macromol. Symp.* **1995**, *93*, 53.
(16) Pearson, D. S.; Graessley, W. W. *Macromolecules* **1978**, *11*, 528.
(17) Moore, C. G.; Watson, W. F. *J. Polym. Sci.* **1956**, *19*, 237. Mullins, L. *J. Appl. Polym. Sci.* **1959**, *2*, 1.
(18) Patel, S. K.; Malone, S.; Cohen, C.; Gillmor, J. R.; Colby, R. H. *Macromolecules* **1992**, *25*, 5241.
(19) Vilgis, T. A.; Boué, F. *Polymer* **1986**, *27*, 1154.
(20) Strauber, E.; Urban, V.; Pyckhout-Hintzen, W.; Richter, D.; Glinka, C. J. *Phys. Rev. Lett.* **1995**, *74*, 4464.
(21) Flory, P. J.; Erman, B. *Macromolecules* **1982**, *15*, 806.
(22) Sharaf, M. A.; Mark, J. E. *Polymer* **1994**, *35*, 740.
(23) Vilgis, T. A.; Erman, B. *Macromolecules* **1993**, *26*, 6657.
(24) Gottlieb, M.; Gaylord, R. J. *Polymer* **1983**, *24*, 1644; *Macromolecules* **1984**, *17*, 2024; *Macromolecules* **1987**, *20*, 130.
(25) Deam, R. T.; Edwards, S. F. *Philos. Trans. R. Soc. A* **1976**, *280*, 317.
(26) Everaers, R. Ph.D. Thesis, University of Bonn, Bonn, Germany, 1994. Everaers, R.; Kremer, K. *in preparation.*
(27) Flory, P. J.; Rehner, J. *J. Chem. Phys.* **1943**, *11*, 512.
(28) Graessley, W. W. *Macromolecules* **1975**, *8*, 186, 865.
(29) Rubberlike materials can be considered to be incompressible with a Poisson ratio of $^1/_2$, since their bulk modulus is that of a liquid. We always consider the standard volume-conserving uniaxial elongation

$$\hat{\lambda} = \begin{pmatrix} \lambda & & \\ & 1/\sqrt{\lambda} & \\ & & 1/\sqrt{\lambda} \end{pmatrix}$$

(30) Kremer, K.; Grest, G. S. *J. Chem. Phys.* **1990**, *92*, 5057; **1991**, *94*, 4103 (Erratum).
(31) Everaers, R.; Kremer, K. *Comput. Phys. Commun.* **1994**, *81*, 19.
(32) Ball, R. C.; Edwards, S. F. *Macromolecules* **1980**, *13*, 748.
(33) Erman, B.; Monnerie, L. *Macromolecules* **1989**, *22*, 3342.
(34) Iwata, K. *J. Chem. Phys.* **1982**, *76*, 6363.
(35) Graessley, W. W.; Pearson, D. S. *J. Chem. Phys.* **1977**, *66*, 3363.
(36) Ball, R. C.; Doi, M.; Edwards, S. F.; Warner, M. *Polymer* **1981**, *22*, 1010.
(37) Higgs, P. G.; Ball, R. C. *Europhys. Lett.* **1989**, *8*, 357.
(38) Doi, M.; Edwards, S. F. *The Theory of Polymer Dynamics*; Oxford University Press: Oxford, U.K., 1986.
(39) Edwards, S. F.; Vilgis, T. A. *Rep. Prog. Phys.* **1988**, *51*, 243.
(40) Heinrich, G.; Straube, E.; Helmis, G. *Adv. Polym. Sci.* **1988**, *85*, 34.

MA9501508